Int. J Heat Mass Transfer. Vol. 13, pp. 263–274. Pergamon Press 1970. Printed in Great Britain

CONVECTIVE HEAT TRANSFER AT THE SURFACE OF A CORONA ELECTRODE

MYRON ROBINSON*

Research-Cottrell, Bound Brook, New Jersey 08805, U.S.A.

(*Received* 6 *June* 1969)

Abstract—It is shown experimentally that a corona discharge established on a heated wire immersed in a cooler gas enhances heat transfer from the wire to the gas, ostensibly by disrupting the boundary layer about the wire. Under circumstances of otherwise natural convection from a 500°F wire, for example, corona is observed to raise the heat-transfer rate fourfold. In forced flow at velocities up to at least 90 ft/s, heat-transfer enhancement due to corona is less marked, but still significant. At zero forced draft the increase in Nusselt number ΔNu resulting from the corona is shown to be a function of the product $Es \cdot Pr$, where Es is a dimensionless electromechanical number and Pr is the Prandtl number. Possible applications of corona-enhanced heat transfer include a heat exchanger for use in a zero-gravity environment in the absence of forced draft, and an apparatus for remotely controlling the nature of the boundary layer, and with it, aerodynamic drag and rates of heat or mass transfer.

NOMENCLATURE

A, gas constant [V/m];

B, gas constant [$V/m^{\frac{1}{2}}$];

b_+, mobility of positive charge carriers [(m/s)/(V/m)];

b_-, mobility of negative charge carriers [(m/s)/(V/m)];

b_0, positive ion mobility at reference temperature T_0 [(m/s)/(V/m)];

c, specific heat of gas at constant pressure [J/kg-°K];

E, electric field intensity, [V/m];

Es, Es', Es'', Esther number, dimensionless. equations (35), (23), (24);

F, force per unit volume of gas [N/m^3];

F_1, bouyant force per unit volume [N/m^3];

F_2, coulomb force per unit volume, [N/m^3];

g, acceleration due to gravity [m/s^2];

Gr, Grashof number, dimensionless, equation (21);

i_c, corona current [A]

j, total linear corona current density [A/m];

j_+, positive linear current density [A/m];

j_-, negative linear current density [A/m];

j'_+, positive areal current density [A/m^2];

j'_-, negative areal current density [A/m^2];

k, thermal conductivity of gas [W/m-°K];

L, characteristic linear dimension [m];

Nu, Nusselt number, dimensionless, equation (25);

$(Nu)_{nat}$, Nusselt number due to natural convection, dimensionless;

ΔNu, change of Nusselt number due to corona, dimensionless;

P, gas pressure [N/m^2];

P_h, heating power dissipated by wire with corona [W];

* Present address: Health and Safety Laboratory, U.S. Atomic Energy Commission, 376 Hudson Street, New York, N.Y. 10014, U.S.A.

P_0, heating power dissipated by wire without corona [W];
Pr, Prandtl number, dimensionless, equation (22);
$\dot{q}$, heat-transfer rate per unit area of wire by all mechanisms [W/m^2];
$\dot{q}_b$, heat-transfer rate per unit area of wire by natural convection [W/m^2];
$\dot{q}_c$, heat-transfer rate per unit area of wire by conduction [W/m^2];
$\Delta\dot{q}$, heat-transfer rate per unit area of wire by electric-wind convection [W(m^2];
r, wire radius [m];
R, tube radius [m];
Re, Reynolds number, dimensionless equation 12
T, absolute temperature of gas [°K];
T_f, mean absolute film temperature [°K];
T_0, 273°K, an absolute reference temperature;
T_w, absolute wire temperature [°K];
T_∞, absolute temperature of incoming gas [°K];
ΔT, absolute temperature differential across boundary film [°K];
v, gas velocity [m/s];
v_e, electric-wind velocity [m/s];
v_+, velocity of positive charge carriers [m/s];
v_-, velocity of negative charge carriers [m/s];
V_c, corona-starting voltage [V];
z, wire length [m];
β, volume coefficient of thermal expansion of gas [°K^{-1}];
δ, gas density relative to standard condition, dimensionless;
η, gas viscosity [dkP];
ρ, gas density [kg/m^3];
ρ_+, positive charge density [C/m^3];
ρ_-, negative charge density [C/m^3];

1. INTRODUCTION

THE LUMINOUS sheath enveloping a corona-discharge electrode in a gas is a zone of intense electrical and mechanical activity i.e. ions and neutral molecules carried along by them (electric wind) are continuously swept in and out of the region of glow adjacent to the electrode surface. If the corona electrode is heated to a temperature above that of the gas in which it is immersed, one might plausibly expect more efficient heat transfer to the gas in consequence of the disruption of the boundary film by the discharge and the convective action of the electric wind.

This mechanism of heat-transfer enhancement utilizing a corona discharge is to be distinguished from the electrostrictive method of Senftleben and Braun [1] and their followers [2–4], from the electric-wind technique of Burke [5], Velkoff [6–8] and Marco [8], and from the ionic-current process Mixon [9], Bhand [10] and their coworkers. The Senftleben–Braun effect obtains by virtue of the fact that the dielectric constant of the convecting fluid is a function of its mass density, i.e. the phenomenon is electrostrictive rather than simple coulombic, and there is no corona. The Burke–Velkoff–Marco method, on the other hand, does employ corona, but in this instance the corona wind is directed from its electrode of origin against the heat-transfer surface. In the approach discussed in this paper, it is an essential feature that the corona discharge be established at the heat-transfer surface itself, the object being the breakup—at least in part—of the boundary film by fluid activity in or near the region of corona glow. The investigations of Mixon, Bhand *et al.* deal with the influence of electrolytic bubble evolution in the cooling of a heated electrode.

That the thermal boundary layer at a hot surface is, in fact, modified by a corona discharge close to the surface has been graphically demonstrated by Franke using an interfero-

metric technique [11]. The resultant heat-transfer enhancement is attributed specifically to the action of counterrotating vortex rolls. These are produced by corona from parallel discharge wires of alternating polarity mounted on the dielectric heat-transfer surface used in Franke's experiments.

It is possible that corona-induced vortices are likewise responsible for boundary layer disruption in the experiments described in this paper. Against this, however, we have the observations that circulatory convection does not seem to be an identifiable feature of the electric wind of the monopolar corona discharge. This question, which is far from settled, has been considered from time to time in the literature on electrostatic precipitation to which the interested reader is referred [12–16].

2. EXPERIMENTAL APPARATUS AND METHOD

The experimental apparatus is shown schematically in Fig. 1. A platinum wire 0·02 in. dia. and 12 in. long is mounted coaxially in a metal tube of the same length and $2\frac{3}{32}$ in. i.d. Each end of the tube is jointed to a Plexiglas insulator the upper insulator supporting a T-shaped member from which the wire hangs, and the lower insulator, a corresponding member which centers the wire, yet permits it to be pulled taut in case of thermal expansion. The upper and lower and vertical wire supports (shrouds) are of iron $\frac{1}{8}$ in. dia. This choice of diameter—larger than that of the wire—ensures that the corona discharge will be confined to the wire alone, over the entire range of corona voltages employed. Despite the need to minimize the electrical resistance of connecting leads in the low-voltage heater circuit external to the platinum wire, iron rather than copper shrouds are used in order to reduce heat loss by conduction from the ends of the wire to the shrouds.

Heating power is supplied to the wire by a 6 V storage battery and regulated by a potentiometer as shown. Instrumentation is provided for measuring the heater current through the platinum wire and the voltage across it. The

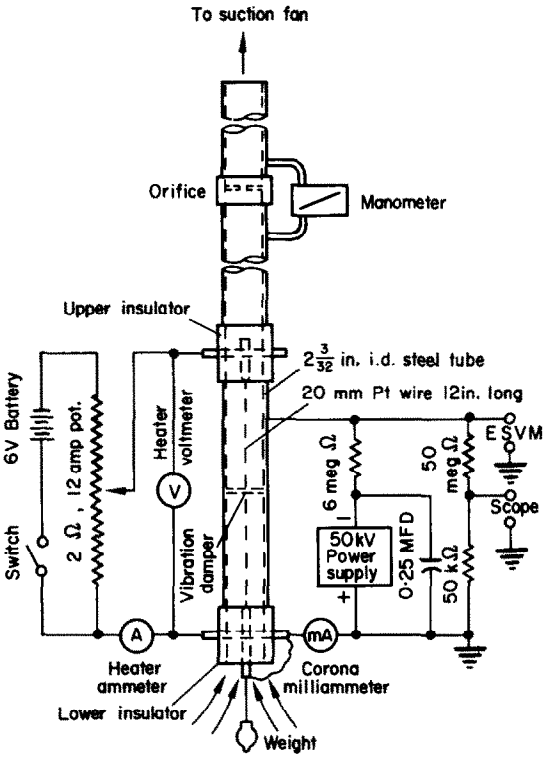

FIG. 1. Experimental apparatus showing coaxial wire-tube electrodes, heating and corona power circuits, and instrumentation.

temperature of the wire can be determined at any heating-power input by relating the wire resistance (as found from the voltage/current ratio) to the temperature, by means of a previously obtained calibration curve. Platinum is preferred for the heated wire because that metal shows no temperature-resistance hysteresis over repeated cycling, has a much greater electrical resistivity than the copper used elsewhere in the circuit, and possesses a satisfactorily high temperature coefficient of resistivity. In addition, the emissivity of platinum wire is low, thereby minimizing radiative heat losses. d.c. heating power is used to prevent the inductive reactance of the iron shrouds—present with a.c.—from masking the small changes in platinum-wire temperature that it is desired to measure.

Earlier investigators of heat transfer from an

electrically heated wire [1, 2, 4, 10] employed a far more sensitive temperature-measuring circuit, one in which the hot wire comprised one arm of a Wheatstone or Kelvin bridge. This arrangement, although also desirable in the present case, proved impractical: resistance-bridge circuitry does not readily lend itself to the relatively high currents required to attain the wire temperatures needed in this study.

The resistance of the connecting leads, shrouds and junctions of the heating circuit is less than 1 percent of that of the platinum wire. Wire-temperature measurements are almost always reproducible to within $\pm 20°F$ over the range 75–1500°F.

In order that the heating-circuit controls be easily accessible, the platinum wire is grounded and the tube raised to high potential. A discharge of positive polarity (i.e. tube at negative potential) is selected for two reasons: (1) The Crookes dark space adjacent to the electrode surface in the negative corona conceivably corresponds to a zone of relative aerodynamic quiescence, and (2) the more evenly distributed positive corona possibly yields a more uniform temperature distribution over the surface of the discharge electrode. No tests were performed to determine whether either of the foregoing effects was significant. A 6 MΩ current-limiting resistor between the high-voltage power supply and the corona wire protect the wire from breakage in the event of sparkover. High voltage is read on an electrostatic voltmeter, and the voltage is monitored by an oscilloscope to insure d.c. of negligible ripple.

A ceramic rod, dia. $\frac{1}{8}$ in., mounted at right angles to the wire at midlength, serves as a vibration damper suppressing wire oscillation that tends to occur for certain combinations of wire tension and electrostatic force.

In this paper, the term "forced convection" refers to that component of convection arising from a pressure differential externally applied to the wire-tube system. "Internal convection", on the other hand, designates convection due to forces originating within the wire-tube system, namely natural convection and convection produced by the electric wind.

All tests were carried out in room air (75°F). The full ductwork shown in Fig. 1 was used in experiments in forced convection; in experiments in internal convection that portion of the apparatus above the upper insulator was removed.

3. THEORY

The fundamental relations governing the rate of heat transfer from the wire to the gas in the system under consideration are the respective Navier–Stokes and heat-transfer equations

$$\mathbf{F} - \rho \mathbf{v} \cdot \nabla \mathbf{v} - \nabla p + \eta \nabla^2 \mathbf{v} = 0 \tag{1}$$

and

$$c\rho \mathbf{v} \cdot \nabla T - k \nabla^2 T = 0. \tag{2}$$

(MKS units will be used throughout the development of the theory. Experimental data, however, will sometimes be reported in mixed units.). We assume in equations (1) and (2) that the stationary state has been attained, that the gas is an essentially incompressible fluid of uniform viscosity, and that the thermal effects of radiation, adiabatic compression, and internal friction are negligible relative to conduction and convection.

The body force/volume $\mathbf{F}$ consists of bouyant and electrostatic components. The bouyant force/volume $\mathbf{F}_1$ due to a thermally induced density variation $\Delta\rho$ is given by

$$\mathbf{F}_1 = \Delta\rho \mathbf{g} = \rho\beta\Delta T \mathbf{g} = \rho \frac{\Delta T}{T} \mathbf{g}. \tag{3}$$

A volume of gas containing positive and negative charges of respective densities ρ_+ and ρ_- and acted upon by an electric field of intensity $\mathbf{E}$ experiences a force per unit volume

$$\mathbf{F}_2 = (\rho_+ + \rho_-)\mathbf{E} \tag{4}$$

Assuming that the velocities of the respective positive and negative charge carriers v_+ and v_-

are not materially influenced by convection currents we may write

$$\mathbf{v}_+ = b_+\mathbf{E} \tag{5}$$

$$\mathbf{v}_- = b_-\mathbf{E}. \tag{6}$$

(The determination of meaningful values of mobility adjacent to the discharge electrode presents a number of problems. This point will be returned to later.) The respective positive and negative areal current densities $\mathbf{j}'_+$ and $\mathbf{j}'_-$ at any point in the interelectrode space are given by

$$\mathbf{j}'_+ = \rho_+\mathbf{v}_+ = \rho_+ b_+ \mathbf{E} \tag{7}$$

$$\mathbf{j}'_- = \rho_-\mathbf{v}_- = \rho_- b_- \mathbf{E} \tag{8}$$

whence

$$\mathbf{F}_2 = \frac{\mathbf{j}'_+}{b_+} + \frac{\mathbf{j}'_-}{b_-}. \tag{9}$$

Of the terms $\mathbf{j}'_-$, ρ_-, $\mathbf{v}_-$ representing negative charge, $\mathbf{j}'_-$ is a positive quantity and the others are negative.

Equation (1) now takes the form

$$\rho\frac{\Delta T}{T}\mathbf{g} + \left(\frac{\mathbf{j}'_+}{b_+} + \frac{\mathbf{j}'_-}{b_-}\right) - \rho\mathbf{v}\cdot\nabla\mathbf{v} - \nabla p + \eta\nabla^2\mathbf{v}. \tag{10}$$

An exact solution of equations (2) and (10) subject to existing constraints is not feasible. Instead, as is usual in such cases, we obtain useful results by employing methods of similarity, in a manner analogous to the treatment of electrostrictive heat transfer by Kronig and Schwarz [2]. It is assumed that considerations of similarity can be extended to the corona discharge, and that stepwise ionization, photoionization, and other mechanisms for which similarity does not hold [17a], do not play dominant roles in the process.

Similarity conditions for flow require that at corresponding points for two geometrically similar systems 1 and 2

$$\frac{[\rho(\Delta T/T)\,\mathbf{g}]_1}{[\rho(\Delta T/T)\,\mathbf{g}]} = \frac{[(\mathbf{j}'_+/b_+) + (\mathbf{j}'_-/b_-)]_1}{[(\mathbf{j}'_+/b_+) + (\mathbf{j}'_-/b_-)]_2} = \frac{(\rho\mathbf{v}\cdot\nabla\mathbf{v})_1}{(\rho\mathbf{v}\cdot\nabla\mathbf{v})_2} = \frac{(\nabla p)_1}{(\nabla p)_2} = \frac{(\eta\nabla^2\mathbf{v})_1}{(\eta\nabla^2\mathbf{v})_2}. \tag{11}$$

Taking L as a characteristic linear dimension of the system, we have

$$\frac{[\rho(\Delta T/T)\,g]_1}{[\rho(\Delta T/T)\,g]_2} = \frac{\overset{\text{I}}{[(\mathbf{j}'_+/b_+} + \overset{\text{II}}{\mathbf{j}'_-/b_-)]_1}}{[(\mathbf{j}'_+/b_+ + \mathbf{j}'_-/b_-)_2} = \frac{\overset{\text{III}}{(\rho v^2/L)_1}}{(\rho v^2/L)_2} = \frac{\overset{\text{IV}}{(p/L)_1}}{(p/L)_2} = \frac{\overset{\text{V}}{(\eta v/L^2)_1}}{(\eta v/L^2)_2}. \tag{12}$$

Ratios I and V may be rewritten in the dimensionless form

$$\left(\frac{\rho\Delta T g L^2}{T\eta v}\right)_1 = \left(\frac{\rho\Delta T g L^2}{T\eta v}\right)_2. \tag{13}$$

Similarly, rearranging III and V, we obtain the Reynolds number Re

$$\left(\frac{\rho v L}{\eta}\right)_1 = \left(\frac{\rho v L}{\eta}\right)_2. \tag{14}$$

Ratios III and IV yield the pressure coefficient

$$\left(\frac{p}{\rho v^2}\right)_1 = \left(\frac{p}{\rho v^2}\right)_2. \tag{15}$$

And finally, from ratios II and V,

$$\left[\left(\frac{j'_+}{b_+} + \frac{j_-}{b_-}\right)\frac{L^2}{\eta v}\right]_1 = \left[\left(\frac{j'_+}{b_+} + \frac{j'_-}{b_-}\right)\frac{L^2}{\eta v}\right]_2 \tag{16}$$

For similarity of temperature fields, it follows from equation (2) that

$$\frac{(c\rho v T/L)_1}{(c\rho v T/L)_2} = \frac{(kT/L^2)_1}{(kT/L^2)_2}, \tag{17}$$

or, in dimensionless terms,

$$\left(\frac{c\rho v L}{k}\right)_1 = \left(\frac{c\rho v L}{k}\right)_2. \tag{18}$$

We now confine our attention to cooling processes resulting only from the effects of bouyancy and the electric wind, i.e. zero forced draft. In such a case we may plausibly assume that the gas velocity is sufficiently small so that the inertial term $\rho\mathbf{v}\cdot\nabla\mathbf{v}$ (whence $\rho v^2/L$) involving the square of the velocity in the equation of motion may be neglected. We note further

that since the gas velocity is not determined by an externally impressed pressure gradient, both pressure and velocity adjust themselves automatically under the action of internal electric and bouyant forces. Consequently, we drop the pressure term from consideration and eliminate v from the remaining relevant dimensionless groups given by equations (13), (16) and (18). Thus, equations (13) and (18) and equations (16) and (18) yield, respectively,

$$\left(\frac{\rho^2 \Delta T g L^3}{T\eta^2} \cdot \frac{c\eta}{k}\right)_1 = \left(\frac{\rho^2 \Delta T g L^3}{T\eta^2} \cdot \frac{c\eta}{k}\right)_2 \quad (19)$$

and

$$\left[\left(\frac{j'_+}{b_+} + \frac{j'_-}{b_-}\right)\frac{\rho L^3}{\eta^2} \cdot \frac{c\eta}{k}\right]_1 = \left[\left(\frac{j'_+}{b_+} + \frac{j'_-}{b_-}\right)\frac{\rho L^3}{\eta^2} \times \frac{c\eta}{k}\right]_2. \quad (20)$$

The two foregoing equations contain three dimensionless numbers: that of Grashof

$$Gr = \frac{\rho^2 \Delta T g L^3}{T\eta^2}, \quad (21)$$

Prandtl

$$Pr = \frac{c\eta}{k}, \quad (22)$$

and an electromechanical parameter which we designate the Esther number

$$Es' = \left(\frac{j'_+}{b_+} + \frac{j'_-}{b_-}\right)\frac{\rho L^3}{\eta^2}. \quad (23)$$

It is convenient to use the currents per unit length of wire j_+ and j_- in place of the respective areal current densities j'_+ and j'_-. The Esther number is then modified to

$$Es'' = \left(\frac{j_+}{b_+} + \frac{j_-}{b_-}\right)\frac{\rho L^2}{\eta^2}. \quad (24)$$

Similar temperature fields yield identical Nusselt numbers

$$Nu = \frac{\dot{q}L}{k\,\Delta T}. \quad (25)$$

In the absence of forced draft and the subsequent neglect of the inertial term in the equation of motion, products of velocity components and their derivatives no longer occur. Thus, both equations (1) and (2) are linear differential equations, and the rule for writing the general solution as the sum of particular solutions leads us to expect

$$Nu = f(Gr \cdot Pr) + g(Es'' \cdot Pr). \quad (26)$$

Taking the characteristic length L to be the wire diameter d, the difference in the Nusselt numbers with and without corona current, but under otherwise unchanged conditions, is given by

$$\Delta Nu = \frac{\Delta\dot{q}d}{k\,\Delta T} = g(Es'' \cdot Pr). \quad (27)$$

The extent of heat-transfer enhancement by corona is perhaps more directly illustrated by considering, in place of ΔNu, the ratio P_h/P_0. This ratio may be written in terms of the component contributions to over-all heat transfer

$$\frac{P_h}{P_0} = \frac{\Delta\dot{q} + \dot{q}_b + \dot{q}_c}{\dot{q}_b + \dot{q}_c} = \frac{\dot{q}}{\dot{q}_b + \dot{q}_c}. \quad (28)$$

It follows that

$$\frac{P_h}{P_0} = 1 + \frac{\Delta Nu}{(Nu)_{\text{nat}}} = 1 + \frac{g(Es'' \cdot Pr)}{f(Gr \cdot Pr)} \quad (29)$$

where $(Nu)_{\text{nat}}$ is the Nusselt number due to natural convection.

Equation (10), for the case of forced draft, is nonlinear and not so easily handled. Neglecting the cooling effect of natural convection relative to that of forced draft and the electric wind, we may write

$$Nu = F(Re, Es'', Pr) \quad (30)$$

where

$$Re = \frac{\rho L v}{\eta}. \quad (31)$$

4. EXPERIMENTAL RESULTS AND DISCUSSION

4.1 *Temperature-dependent variables*

Contrary to the procedure followed by Kronig and Schwarz [2], the values of the temperature-dependent variables c, b_+, ρ, η and k were taken at the mean film temperature

$$T_f = \frac{T_w + T_\infty}{2}. \tag{32}$$

This approach seems reasonable because

1. Corona discharge characteristics are markedly affected by changes in gas temperature close to the wire even though the temperature of the much larger main body of gas changes relatively little. See Fig. 2.

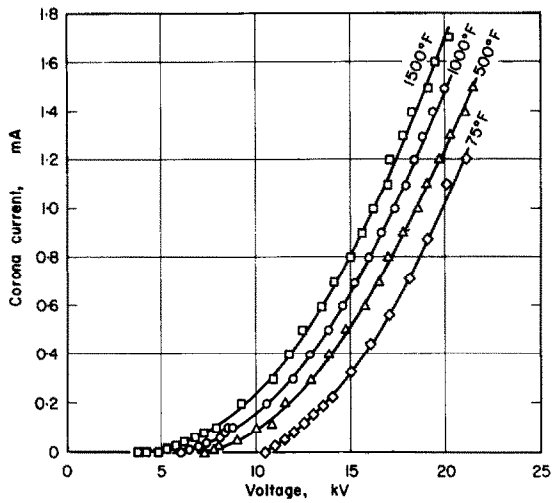

FIG. 2. Effect of the heated discharge wire on corona current–voltage characteristics. The maximum voltage of each curve corresponds to sparkover. There is no forced draft.

2. Corona activity is confined to roughly the same region as the boundary layer, the disruption of which is postulated to be primarily responsible for enhancing heat transfer from the wire.

3. The velocity of the radially divergent electric wind decreases with distance from the corona. Thus, although the electric wind contributes to convection throughout the entire volume of the tube, its effect is expected to be greatest close to the corona sheath.

Assignment of numerical values to the ion mobility presents a particularly knotty problem in the boundary layer, a region of ion instability and intense and (spatially) rapidly varying fields. For a first approximation, we grossly oversimplify and set [17b]

$$b_+ = b_0 \frac{T}{T_0}. \tag{33}$$

In the calculations to follow, b_0 is taken to be $1{\cdot}36 \times 10^{-4}$ (m/s)/(V/m) at $T_0 = 273°K$. It is apparent that since a single gas (air) was investigated, the choice of b_0 does not enter into the present experimental verification of the theory; the essential validity of the temperature dependence of b_+ as given by equation (33), is, however, critical.

The corona-starting voltage V_c for concentric wire-tube electrodes in a gas of uniform relative density δ is given by the expression [18]

$$V_c = (A\delta r + B\sqrt{\delta r}) \ln (R/r). \tag{34}$$

It is consequently to be expected that a decrease in gas density close to the hot wire will depress the corona-starting voltage. As Fig. 2 indicates, V_c for a 1500° wire is less than half of its value at room temperature. Discharge conditions in the greater part of the interelectrode space remain essentially unchanged. The chief effect of the hot wire is, therefore, to be seen in the more-or-less parallel displacement of the current-voltage curves.

4.2 *Calculation of Es*

In the interelectrode volume outside the relatively narrow corona sheath surrounding the positive wire the space charge is unipolar and $j_+ = j$, the total linear current density. Within the active corona region, however, the charge carriers are electrons and positive ions for which $b_- \gg b_+$. Assuming here that j_+ and j_- are effectively of the same order of magnitude, the electronic contribution j_-/b_- in equation (24) can be neglected. Further, assuming that j_+ in the corona is proportional to j (the only current susceptible to direct measurement), we

may rewrite equation (24) in the practically useful form

$$Es = \frac{j\rho L^3}{b_+\eta^2} \tag{35}$$

and replace Es'' by Es in the following discussion.

4.3 *Internal convection*

Experimental data, for internal convection, relating the change of Nusselt number ΔNu to the product $Es \cdot Pr$ [equation (27)] for wire temperatures of 500°, 1000° and 1500°F are given in Fig. 3. The observed points fall in a relatively narrow band, a circumstance all the more remarkable in view of the several questionable assumptions and uncertain approximations employed. A reasonable presumption therefore exists that the theory of internal convection presented is approximately correct, at least in its most essential features.

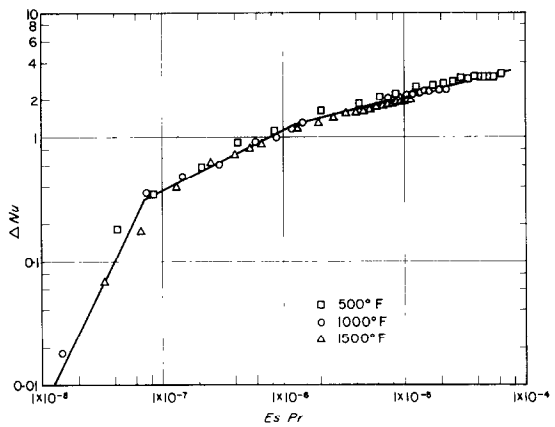

FIG. 3. Change of Nusselt number due to corona cooling in terms of the dimensionless product $Es \cdot Pr$ for zero forced draft.

The curve of Fig. 3 is divided into three rather distinct segments, each apparently responsive to a different cooling mechanism. From left to right we designate the regimes I, II and III

$$\text{I} \quad \Delta Nu = 6{\cdot}6 \times 10^{13} (Es \cdot Pr)^2 \tag{36}$$

$$\text{II} \quad \Delta Nu = 1{\cdot}17 \times 10^{3} (Es \cdot Pr)^{\frac{1}{2}} \tag{37}$$

$$\text{III} \quad \Delta Nu = 38 (Es \cdot Pr)^{\frac{1}{4}}. \tag{38}$$

In regime I the corona discharge is unstable and the current erratic. The lowest limit of ΔNu (for the least measurable corona current) corresponds to the uppermost limit of ΔNu for electrostrictive heat transfer as reported by Kronig and Schwarz [2].

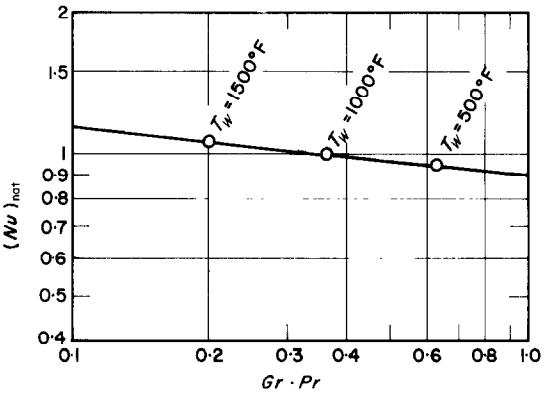

FIG. 4. Nusselt number in natural convection as a function of the dimensionless product $Gr \cdot Pr$.

It turns out (see Fig. 4), over the range of experimental variables examined, that

$$(Nu)_{\text{nat}} = f(Gr \cdot Pr) \approx 1. \tag{39}$$

Equation (29) therefore simplifies to

$$\frac{P_h}{P_0} \approx 1 + \Delta Nu = 1 + g(Es \cdot Pr). \tag{40}$$

It is of interest to consider the heat-transfer enhancement ratio P_h/P_0 in terms of the velocity of the electric wind. Theoretically and experimentally, it has been shown that a suitably constrained, unidirectional electric wind blows with a velocity v_e that is proportional to the square root of the exciting corona current i_c [19]. Regarding $i_c^{\frac{1}{2}}$ as an indicator of a characteristic value of v_e in the present tests, we plot P_h/P_0 vs. $i_c^{\frac{1}{2}}$, obtaining the somewhat curious results shown in Fig. 5.

Regime I is here scarcely observable, but regime II is immediately identifiable as the family of lines given by equation (40) in the form

$$\frac{P_h}{P_0} \approx 1 + (1{\cdot}17 \times 10^{-3}) \left(\frac{\rho d^2 c}{b\eta kz}\right)^{\frac{1}{2}} i_c^{\frac{1}{2}}. \tag{41}$$

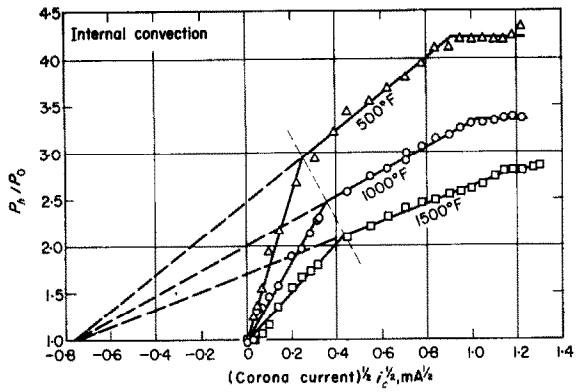

FIG. 5. Heat-transfer enhancement in terms of corona current under conditions of zero forced draft.

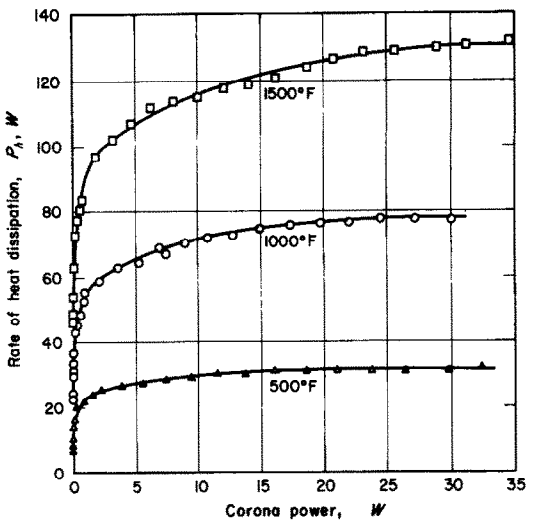

FIG. 6. Effect of corona power on the rate of transfer of thermal energy from a hot discharge wire in the absence of forced draft.

According to equation (38), regime III is non-linear in $i_c^{\frac{1}{2}}$ and is therefore incompatible with the straight-line segments shown for this regime in Fig. 5. Nevertheless, over the interval in question and within the limits of experimental error, the data show that a satisfactory linear approximation (in $i_c^{\frac{1}{2}}$) to equation (38) is possible. The physical basis underlying the common point of intersection at ($P_h/P_0 = 1$, $i_c^{\frac{1}{2}} = -0{\cdot}76$) is not clear.

Still a fourth regime, $P_h/P_0 = \text{const}$, may be identified in Fig. 5. This regime, at the far right of the individual curves, coincides with repeated sparking, the current being determined largely by the external circuit, and so is probably not to be considered in the legitimate corona range. In Fig. 3, the existence of the fourth regime is obscured by the use of a log–log plot.

Figure 5 suggests that, at least approximately, the enhancement ratio P_h/P_0 in terms of electric-wind velocity may be regarded as passing through three stages: proportional, of limited proportionality, and constant.

The rate of heat dissipation (heat transferred) by the wire as a function of corona power (product of corona current and voltage) is shown in Fig. 6. At constant temperatures and low corona-power levels, small increments in corona power are capable of yielding sizable increases in thermal power transferred. To cite an example; at 500°F, 0·5 W of corona power raises the thermal output from about 8 to 20 W, an effective "amplification" of (20–8)/0·5 = 24 times. Similar data, revealing the influence of corona on wire temperature for fixed heating power inputs, are plotted in Fig. 7.

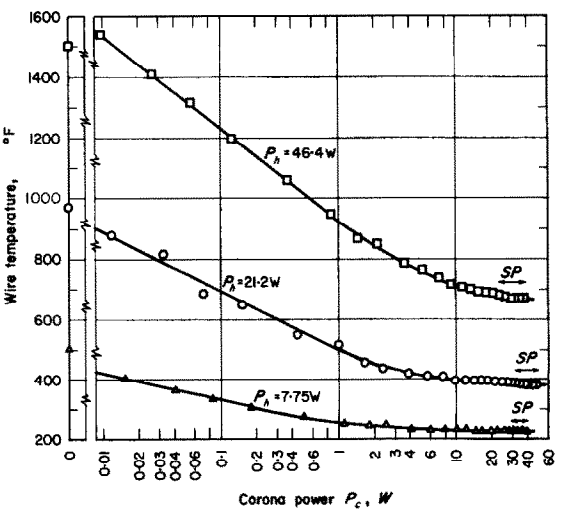

FIG. 7. Effect of the corona discharge on the temperature of a hot wire at zero forced draft. The symbol *SP* designates sparking.

4.4 *Forced convection*

Heat-transfer enhancement observed in the foregoing experiments may be ascribed to both boundary-layer breakup at the wire surface and electric-wind convection throughout the tube. Since electric-wind velocities of the order of ft/s are typical in a system of low back pressure [19], it is not surprising, even in the absence of specific boundary-layer activity, that corona improves heat transfer under circumstances of otherwise free convection. But the contribution of the corona discharge to heat transfer in forced convection is another matter. Under such conditions, Velkoff [6] and Marco [8] have demonstrated that if the tube (the passive electrode with respect to corona) be the heated element, heat-transfer enhancement is insignificant, i.e. in the absence of enhanced boundary-layer breakup, the heat-transfer contribution of the electric wind to existing forced flow is negligible. In the case of heat transfer from the active corona electrode, the situation is quite different. Figure 8 gives the enhancement ratio P_h/P_0 at average air velocities up to 92 ft/s. (P_h is now the heat-transfer rate due to all causes including corona and forced draft, and P_0 is the heat transfer rate from all causes except corona). At velocities of 10 ft/s, corona can more than double the heat-transfer rate, and at velocities of 92 ft/s, a 10 per cent increase in heat transfer is still observed. The data support the view that the corona discharge is an effective mechanism for achieving boundary-layer breakup.

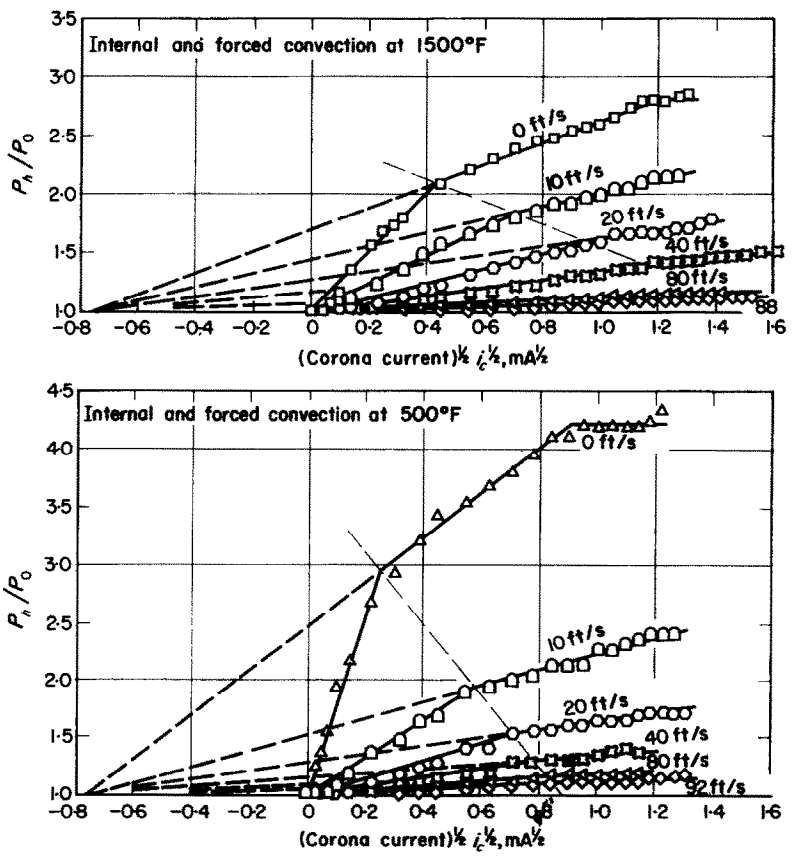

FIG. 8. Heat-transfer enhancement in terms of corona current in the presence of forced draft.

We shall not attempt, in this report, to determine the relation

$$Nu = F(Re, Es, Pr) \tag{42}$$

in explicit form. We observe merely that experimentally Nu is not proportional to a constant power of Re, and that the regions of proportionality, limited proportionality and constancy remain evident in forced draft. The point of intersection of the extrapolated lines of limited proportionality is the same as in internal convection.

5. APPLICATIONS

The following possible applications of corona-induced boundary-layer breakup are suggested.

1. A heat exchanger for use in a zero-gravity environment in the absence of forced draft. Under conditions of zero gravity, natural convection is impossible but corona-induced convection is unaffected.

2. A method for remotely controlling and rapidly varying boundary-layer characteristics, and with it, rates of heat or mass transfer and aerodynamic drag.

3. A heating element that is run relatively cool and yet delivers the same thermal output as a much hotter element without boundary-layer control.

4. A means of modulating the temperature of a heating element dissipating heat at a constant rate.

ACKNOWLEDGEMENT

The author is indebted to Joseph C. Shepard who constructed the experimental equipment and assisted in taking numerous measurements.

REFERENCES

1. H. Senftleben and W. Braun, Der Einfluss elektrischer Felder auf den Wärmestrom in Gasen, *Z. Phys.* **102**, 480–506 (1936).
2. R. Kronig and N. Schwarz, On the theory of heat transfer from a wire in an electric field, *Appl. Scient. Res.* **A1**, 35–46 (1947).
3. P. H. G. Allen, Electric stress and heat transfer, *Br. J. Appl. Phys.* **10**, 347–351 (1959).
4. P. S. Lykoudis and C. P. Yu, The influence of electrostrictive forces in natural thermal conduction, *Int. J. Heat Mass Transfer* **6**, 853–862 (1963).
5. S. P. Burke, Heat transfer, U.S. Patent 1,835,557 (Dec. 8, 1931).
6. H. R. Velkoff, Electrofluidmechanics: Investigation of the effects of electrostatic fields on heat transfer and boundary layers. Technical Documentary Report ASD-TDR-62-650, Wright–Patterson Air Force Base, Ohio (1962).
7. H. R. Velkoff, An exploratory investigation of the effects of ionization on flow and heat transfer with a dense gas. Technical Documentary Report ASD-TDR-63-842, Wright–Patterson Air Force Base, Ohio (1963).
8. S. M. Marco and H. R. Velkoff, Effect of electrostatic fields on free-convection heat transfer from flat plates, *Trans. Am. Soc. Mech. Engrs* Paper No. 63-HT-9 (1963).
9. F. O. Mixon and E. I. Dupont, Effect of electrolytic gas evolution on heat transfer, *Chem. Engng Prog.* **55**, 49–53 (1959).
10. S. C. Bhand, M. S. Gaur and D. V. Gogate, Effect of ionic currents on heat transfer, *Indian J. Phys.* **37**, 185–190 (1963).
11. M. E. Franke, Effects of vortices induced by corona discharge on free-convection heat transfer from a vertical plate, *Trans. Am. Soc. Mech. Engrs* Paper No. 68-WA(HT-9 (1968).
12. R. Ladenburg and W. Tietze, Untersuchungen über die physikalischen Vorgänge bei der sogenannten elektrischen Gasreinigung: Die Wirkung des elektrischen Windes, *Ann. Phys.* **6**, 581–621 (1930).
13. W. Deutsch, Effect of the electric wind in electrical gas purification, *Ann. Phys.* **9**, 249–264 (1931).
14. E. Anderson, On the role of the electric wind in electrical precipitation in gases, *Physics* **3**, 23–28 (1932).
15. J. N. Chubb, W. D. Bamford and J. B. Higham, Experimental studies of airborne particle behavior in corona discharge fields, *Colloquium on Electrostatic Precipitators*, Inst. Elec. Engrs, London (1965).
16. M. Robinson, Turbulent gas flow and electrostatic precipitation, *J. Air Pollut. Control Ass.* **18**, 688–92 (1968).
17. A. von Engel, *Ionized Gases*, 2nd ed., (a) p. 288, (b) p. 115. Oxford (1965).
18. M. Robinson, The corona threshold for coaxial cylinders in air at high pressures, *Trans. Inst. Elect. Electron. Engrs (Power Appl. Systems)* **86**, 185–189 (1967).
19. M. Robinson, Movement of air in the electric wind of the corona discharge, *Trans. Am. Inst. Elect. Engrs* **801**, 143–150 (1961).

TRANSPORT DE CHALEUR PAR CONVECTION À LA SURFACE D'UNE ÉLECTRODE À EFFET COURONNE

Résumé—On montre expérimentalement qu'une décharge par effet couronne établie sur un fil chauffé immergé dans un gaz plus froid augmente le transport de chaleur du fil au gaz, apparemment en brisant la couche limite autour du fil. Dans le cas d'une convection qui serait autrement naturelle à partir d'un fil à 260°C, on observe que l'effet couronne augmente de quatre fois le flux de chaleur. Dans un écoulement forcé à des vitesses allant jusqu'au moins 27,4 m/s, l'augmentation du transport de chaleur due à l'effet couronne est moins marquée, mais encore sensible. Pour un tirage forcé nul, l'augmentation du nombre de Nusselt N_u est une fonction du produit E_s. P, où E_s est un nombre sans dimensions électromécanique et P le nombre de Prandtl. Parmi les applications possibles de l'augmentation du transport de chaleur par effet couronne se trouvent un échangeur de chaleur à employer dans une ambiance à gravité nulle en l'absence de tirage forcé, et un appareil pour contrôler de loin la nature de la couche limite, et par cela, la traînée aérodynamique et les flux de chaleur et de masse.

KONVEKTIVER WÄRMEÜBERGANG AN DER OBERFLÄCHE EINER KORONA-ELEKTRODE

Zusammenfassung—Es wird experimentell gezeigt, dass eine Corona-Entladung an einem beheizten Draht in einem kühleren Gas den Wärmeübergang von Draht an das Gas erhöht, vornehmlich durch das Abreissen der Grenzschicht um den Draht. Unter den Bedingungen der freien Konvektion wurde zum Beispiel an einem 500°F heiseen Draht beobachtet, dass eine Corona-Entladung den Wärmeübergang auf das Vierfache erhöhte. Bei Zwangskonvektion bei Geschwindigkeiten bis zu 90 ft s ist die Steigerung des Wärmeübergangs infolge der Corona weniger ausgeprägt, aber noch deutlich vorhanden. Beim Fehlen von Zwangskonvektion ergab sich das Anwachsen der Nusselt-Zahl *Nu* infolge der Corona als eine Funktion des Produktes: *Es*. *Pr*, wobei *Es* eine dimensionslose elektromechanische Kenngrösse und *Pr* die Prandtl-Zahl darstellt. Mögliche Anwendungen diese Phänomens des erhöhten Wärmeübergangs durch die Corona unfassen: Wärmetauscher in einem schwerkraftfreien Raum beim Fehlen von Zwangskonvektion, Apparate zur Fernkontrolle der Art der Grenzschicht, und in Verbindung damit, des aerodynamischen Widerstandes und des Wärme- oder Stoffübergangs.

КОНВЕКТИВНЫЙ ТЕПЛООБМЕН НА ПОВЕРХНОСТИ КОРОНИРУЮЩЕГО ЭЛЕТРОДА

Аннотация—Экспермент показал, что коронный разряд на нагретой проволочке, помещенной в более холодный газ, увеличивает теплообмен от провочки к газу, явно нарушая пограничный слой вблизи проволочки. Например, при естественной конвекции от проволочки при 500°F замечено, что корона увеличивает интенсивность теплообмена в четыре раза. В условиях вынужденного течения при скоростях до 90 футов/сек наблюдается меньшее, хотя все еще значительное увеличение теплообмена за счет коронного разряда. Показано, что при вынужденной нулевой тяге увеличение числа Нуссельта, обусловленное коронным разрядом, есть функция произведения *Es* . *Pr*, где *Es* есть безразмерное электромеханическое число и *Pr* есть число Прандтля. Возможные приложения увеличения теплообмена за счет коронного разряда включают теплообменник для использования в среде с нулевой гравитацией при отсутствии вынужденного движения, а также аппаратуру для дистанционного контроля характера пограничного слоя, а вместе с тем аэродинамического сопротивления и интенсивности тепло или массообмена.